

High temperature properties of a high-chromium cast iron and its composites fabricated via powder metallurgy process

T. SATOH*, H.-N. LIU, M. SAKAMOTO

National Institute of Advanced Industrial Science and Technology, Kyushu (AIST Kyushu), 807-1 Shuku, Tosu, Saga 841-0052, Japan

E-mail: tomio.sato@aist.go.jp

Y. KAWAKAMI

Industry Technology Center of Saga, 114 Yaemizo, Nabeshima, Saga 849-0932, Japan

High chromium white cast irons are extremely attractive materials for wear-resistant applications in mining and mineral industries, steel producing plants, etc. [1]. Generally, cast irons are designed to consist of a strengthened austenite matrix with uniformly dispersed hard carbides. Over many years, our research group has performed a series of studies on high-Cr cast irons. Consequently, we have discovered a new composition eutectic 36Cr alloy (Fe–36Cr–9Ni–5Mo–2.2C, mass%) with excellent wear-resistance and oxidation-resistance at elevated temperatures [2]. Recently, we

have attempted powder metallurgy (P/M) processing and composite techniques to further improve the high temperature properties of this newly developed 36Cr alloy. This letter reports the hardness, wear-resistance and oxidation-resistance of 36Cr materials (the ingot, the P/M alloy and the alumina powder reinforced composites) in comparison to those of a hypoeutectic 25Cr cast iron (Fe–25Cr–0.5Ni–0.5Mo–2.9C) that is widely used in high-temperature applications.

The 36Cr and 25Cr ingots were prepared using conventional casting. The following process fabricated the

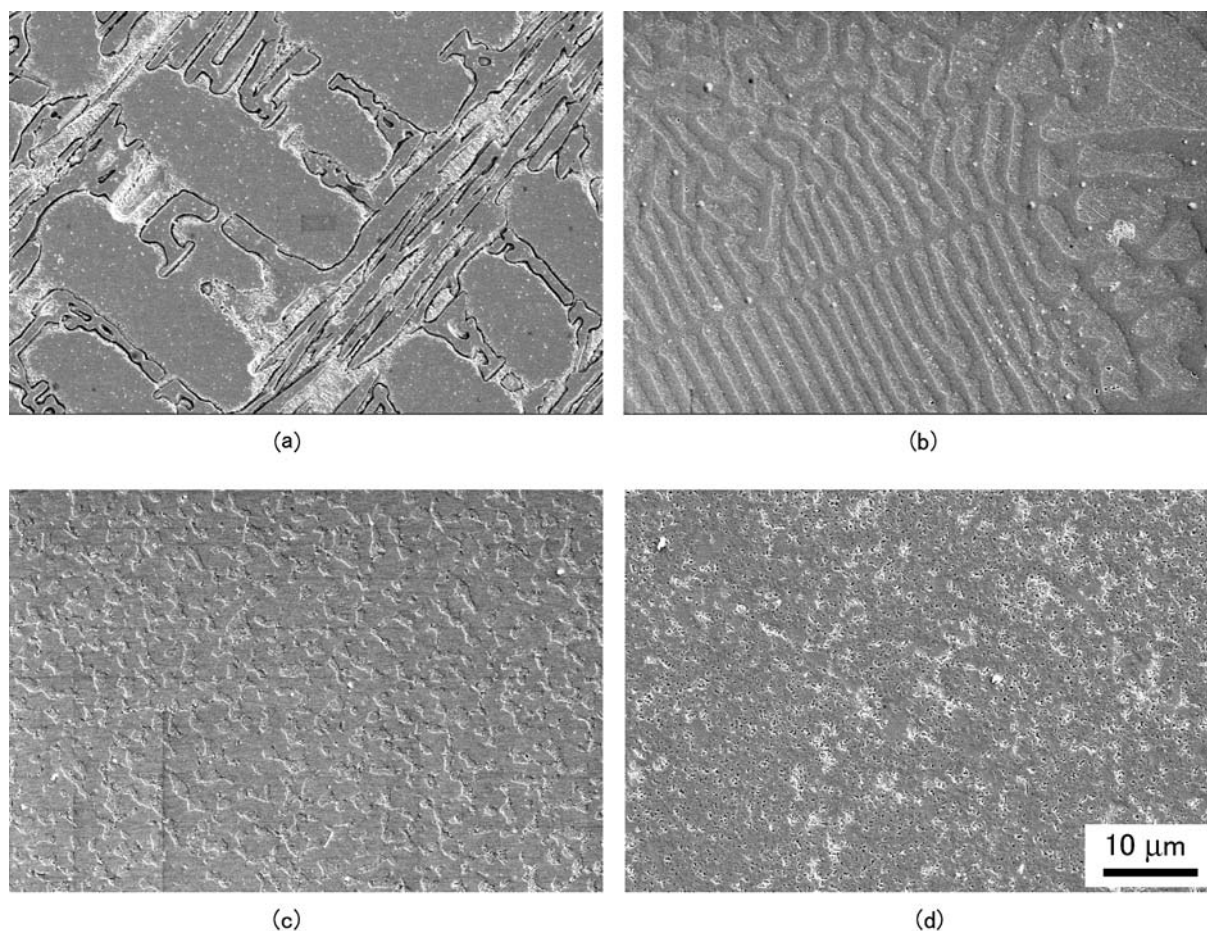


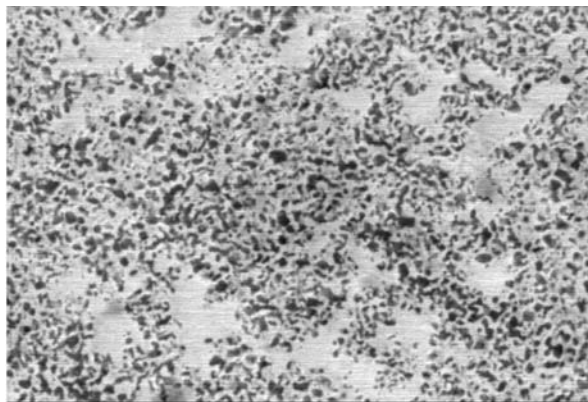
Figure 1 SEM images of: (a) 25Cr ingot, (b) 36Cr ingot, (c) P/M alloy ($V_f = 0\%$), and (d) P/M alloy ($V_f = 30\%$). The specimens were etched in picric acid alcohol.

* Author to whom all correspondence should be addressed.

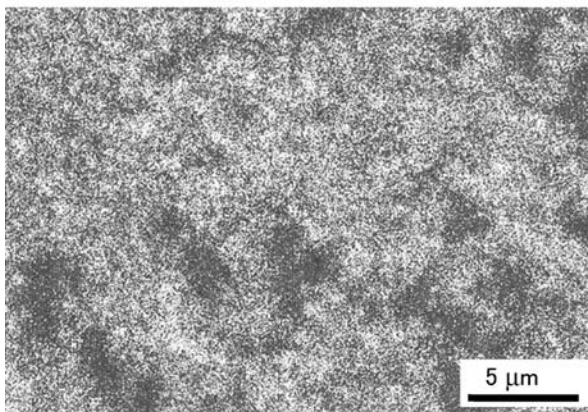
36Cr P/M specimens. (1) Each element powder (which comprises the eutectic 36Cr alloy) with reinforcement was pre-mixed using a V-type blender. The reinforcement was α -Al₂O₃ powder with a mean diameter of 0.4 μ m; the volume fractions (V_f) of the Al₂O₃ powders were 0, 10, and 30%. (2) The pre-mixed powders were subjected to mechanical alloying (MA) with a planetary-type ball mill in argon gas atmosphere for 200 hr. (3) The MA-processed powders were consolidated by spark plasma sintering (SPS) process at 1373 K under a pressure of 50 MPa to form sample disks ($\phi 32 \times 6$ mm). This process, MA followed by SPS, is denoted as MA-SPS process.

The Vickers hardness of the test specimens was measured at room temperature, 773, 873, 973, and 1073 K, respectively, under a load of 49 N in an argon gas atmosphere. The wear test was performed at 923 K for 80 hr using a newly designed low-stress abrasive tester that is described elsewhere [3]. This test method reveals the abrasion-resistance of the test specimen in comparison with that of a standard alloy. In the present study, it is the 25Cr alloy described above. Final results are given by the relative volume loss of the former to that of the latter. The oxidation test was carried out at 1073 K for 100 hr in accordance with the Japanese Industrial Standard (JIS) -Z2281 (the dew point of the air was 303 K, and the flow rate was 0.4 ml/min for 1 mm² of the specimen surfaces) using 20 \times 20 \times 5 mm specimens.

Fig. 1 shows scanning electron microscope (SEM) images of the test specimens. The 25Cr and 36Cr ingots



(a) SEI



(b) Al-K α

Figure 2 SEM/EDX images of P/M alloy ($V_f = 30\%$): (a) SEI and (b) Al-K α .

have typical hypoeutectic and eutectic microstructures, respectively. The 36Cr P/M specimens have homogeneous microstructures that are much finer than that of the 36Cr ingot independent of alumina content.

The distribution behavior of Al₂O₃ in the P/M specimen ($V_f = 30\%$) was examined by energy dispersive X-ray spectroscopy (EDX). Fig. 2 shows SEM/EDX images of the P/M specimen ($V_f = 30\%$). The images show that the Al₂O₃ powder in the P/M specimen is dispersed comparatively homogeneously. No defects are also visible in the P/M specimen.

Fig. 3 shows the Vickers hardness of the test specimens. All 36Cr P/M specimens are harder than the 36Cr ingot at each test temperature. The increase in the Al₂O₃ content considerably increases the hardness of the composites. At 1073 K, the hardness of the P/M specimen of $V_f = 30\%$ is determined to be 584 H_v 5, which is greater than the hardness of the 36Cr ingot and the monolithic P/M specimen at room temperature (RT). Regarding the 25Cr alloy, its RT hardness is vastly greater than those of all the 36Cr materials (the ingot and the P/M alloys), but it decreases rapidly with

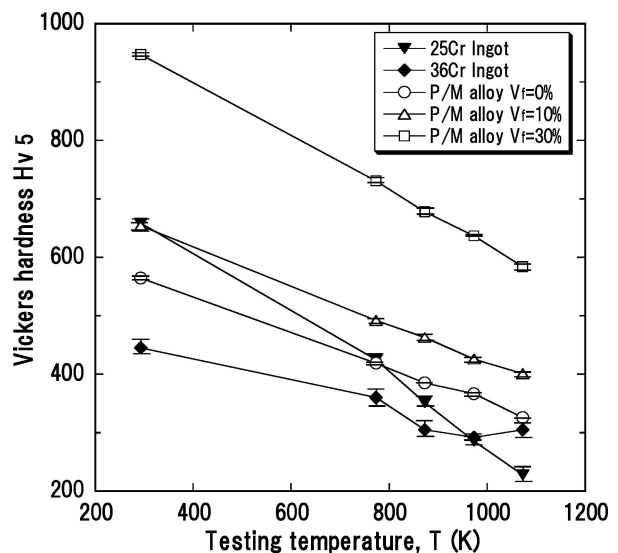


Figure 3 Vickers hardness of test specimens at elevated temperatures.

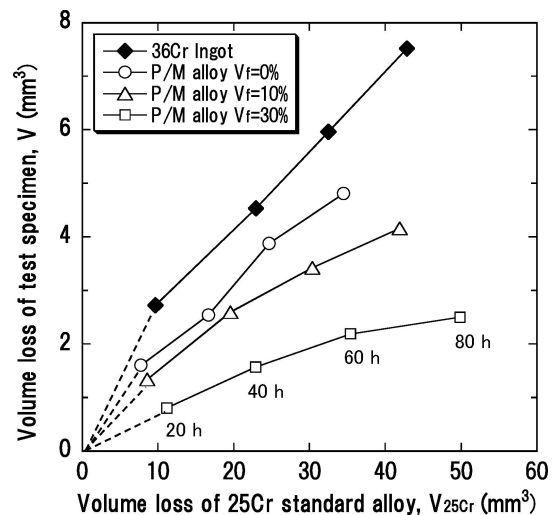


Figure 4 Volume losses of test specimens vs. volume loss of the 25Cr standard alloy at 923 K.

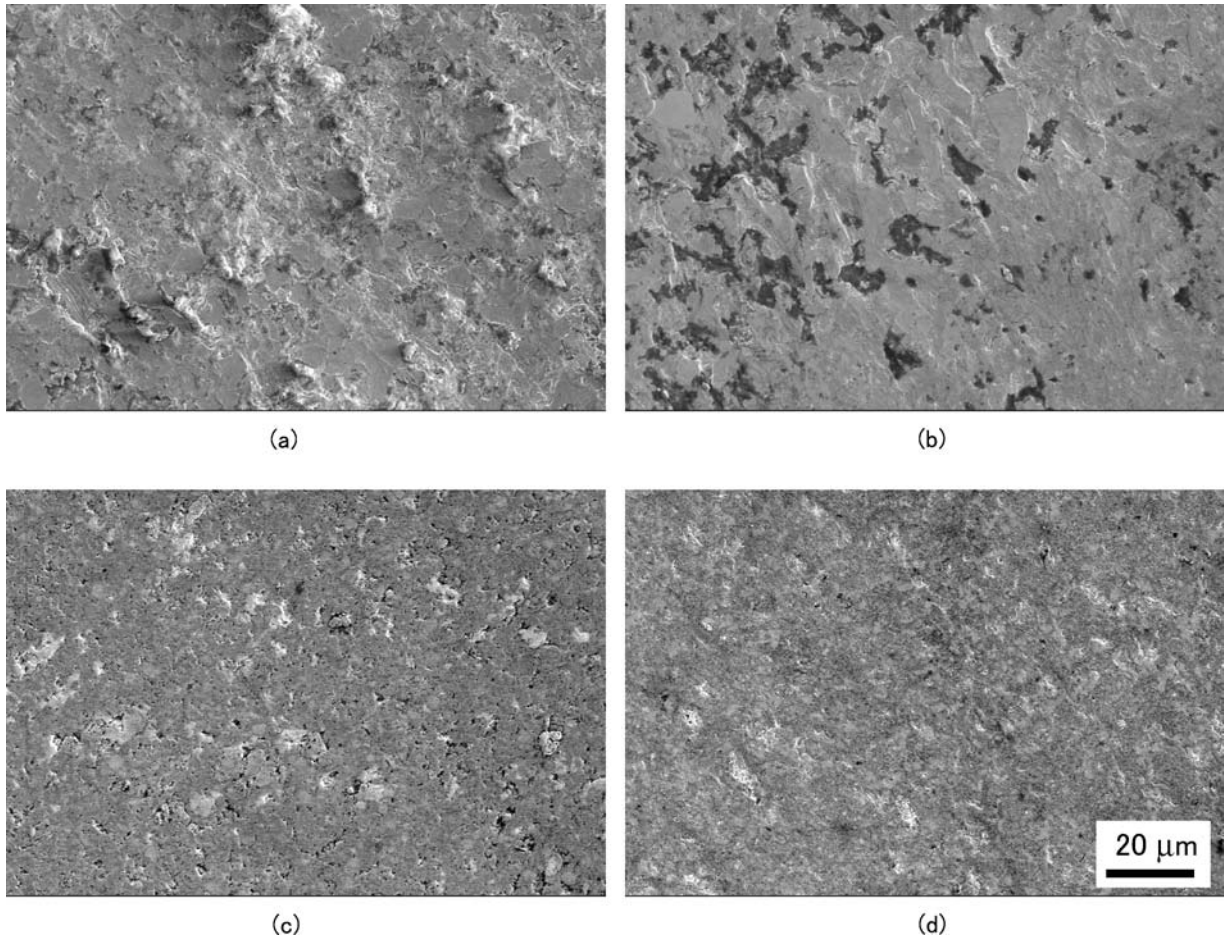


Figure 5 SEM images showing worn surface of: (a) 25Cr ingot, (b) 36Cr ingot, (c) P/M alloy ($V_f = 0\%$), and (d) P/M alloy ($V_f = 30\%$).

increased temperature. At 1073 K, the 25Cr alloy has the lowest hardness among the test materials.

Wear results are plotted in Fig. 4. All 36Cr materials exhibit better abrasion-resistance than the 25Cr alloy. After 80-hr abrasion, the volume loss of the former were less than 20% of that of the latter. Among the 36Cr materials, the P/M specimens are more abrasion-resistant than the ingot. The increase in the Al_2O_3 content markedly increases the abrasion-resistance of the composites, indicating that the high-temperature wear-resistance of the 36Cr materials was further improved by P/M (MA-SPS) process.

Fig. 5 shows the specimens' worn surface morphologies after 80-hr abrasion. The worn surface of the 25Cr ingot shows a relatively rough surface, which is attributable to its microstructure. The primary γ -phase is more worn than the eutectic phase because the γ -phase is softer than the eutectic phase at the test temperature. The 36Cr ingot also presents a worn surface with roughness, whereas the 36Cr P/M specimens have outstanding smooth worn surfaces in comparison with those of the 25Cr and 36Cr ingots. The worn surface roughness (arithmetical mean roughness, R_a) was the 25Cr ingot: $1.33 \mu m$, the 36Cr ingot: $1.18 \mu m$, the P/M specimens of $V_f = 0\%$: $0.10 \mu m$, and the P/M specimen of $V_f = 30\%$ were $0.11 \mu m$, respectively. The P/M specimens exhibit an extremely smooth and refined worn surface.

Fig. 6 shows oxidation results. The mass gains of all the 36Cr materials are much less than that of the 25Cr

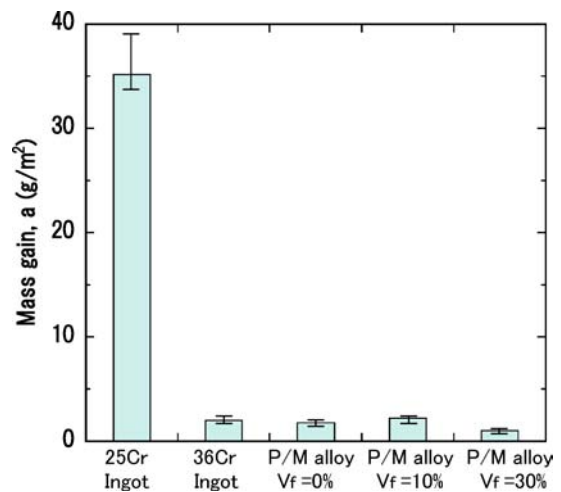


Figure 6 Mass gains of test specimens after oxidation at 1073 K for 100 hr.

alloy, emphasizing their excellent oxidation-resistance. Moreover, among the 36Cr materials, the P/M specimen of $V_f = 30\%$ is the most oxidation-resistant. According to the morphology of oxidized surface shown in Fig. 7, the surface of the 25Cr alloy shows remarkable unevenness with whisker-like oxide crystals in eutectic regions. X-ray diffraction analysis was employed for identification of the oxidized surfaces. The analysis results indicated that the oxidized surface of the 25Cr ingot consisted of Fe_2O_3 and that the oxide formed on

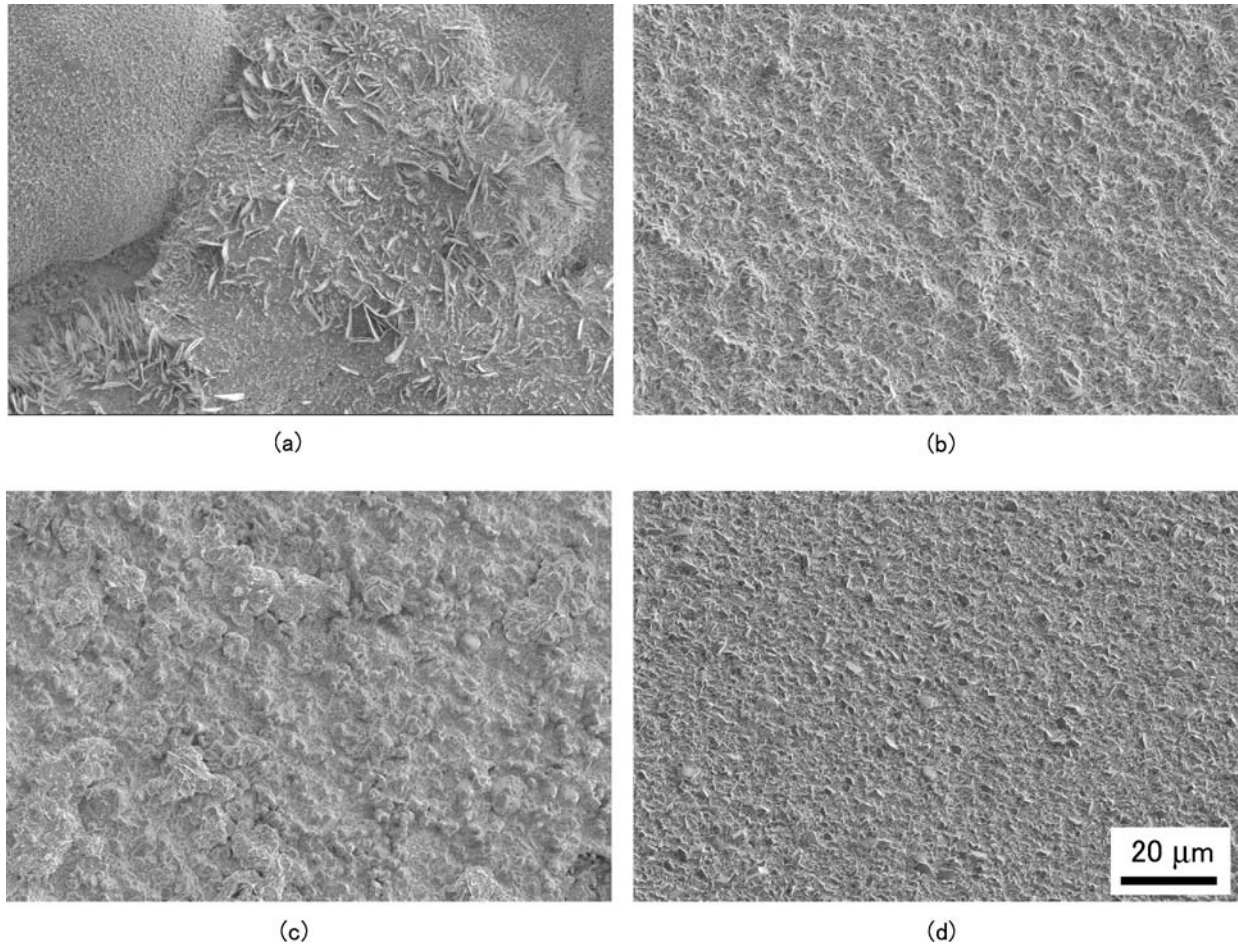


Figure 7 SEM images showing oxide surface of: (a) 25Cr ingot, (b) 36Cr ingot, (c) P/M alloy ($V_f = 0\%$), and (d) P/M alloy ($V_f = 30\%$).

the surfaces of the 36Cr materials was Cr_2O_3 . The peak of Al_2O_3 was also observed for the P/M specimen containing 30 vol% alumina. Regarding the 36Cr materials, all oxidized specimens are extremely smooth; the P/M specimen of $V_f = 30\%$ has the finest oxide surface. The oxide surface roughnesses, R_a , of the 25Cr ingot, 36Cr ingot, P/M specimens of $V_f = 0\%$ and P/M specimen of $V_f = 30\%$ were 5.12, 0.32, 0.67, and $0.15 \mu\text{m}$, respectively. The P/M specimen of $V_f = 30\%$ shows an extremely smooth and refined oxide surface.

In conclusion, the newly developed eutectic 36Cr cast alloy displays vastly better high-temperature abrasion-resistance and oxidation-resistance than the 25Cr cast alloy. The properties of this 36Cr alloy can

be further improved through P/M processing (MA-SPS processing).

References

1. C. P. TONG, T. SUZUKI and T. UMEDA, *Jpn. Foundry Eng. Soc.* **62** (1990) 925.
2. M. SAKAMOTO, S. AKIYAMA, T. SATOH, A. KITAHARA, K. OGI and M. NOMURA, *Jpn. Patent*. Patent No. 3434496 (May 30, 2003).
3. H.-N. LIU, M. SAKAMOTO, M. NOMURA and K. OGI, *Wear* **250** (2001) 71.

Received 25 August
and accepted 19 November 2004